ELSEVIER

Journal of Structural Geology 27 (2005) 1095–1112

JOURNAL OF STRUCTURAL GEOLOGY

www.elsevier.com/locate/jsg

Brittle fractures and ductile shear bands in argillaceous sediments: inferences from Oligocene Boom Clay (Belgium)

B. Dehandschutter[a,*], S. Vandycke[b], M. Sintubin[a], N. Vandenberghe[c], L. Wouters[d]

[a]*Geodynamics & Geofluids Research Group, Katholieke Universiteit Leuven, Redingenstraat 16, 3000 Leuven, Belgium*
[b]*Géologie Fondamentale et Appliquée, Faculté Polytechnique de Mons, 9, rue de Houdain, 7000 Mons, Belgium*
[c]*Stratigraphy Group, Katholieke Universiteit Leuven, Redingenstraat 16, 3000 Leuven, Belgium*
[d]*ONDRAF/NIRAS, Kunstlaan 14, 1210 Brussels, Belgium*

Received 20 December 2003; received in revised form 17 July 2004; accepted 31 August 2004
Available online 29 June 2005

Abstract

Fractures, from vertical joints to micro-scale slickensides, are common in many muds and mudstones. Their origin and formation mechanism remains enigmatic because of the rock–soil transitional behaviour of argillaceous sediments. However, they can have an important impact on the fluid-flow properties and mechanical strength of the rock. The nature of small-scale fractures studied in the field and in the laboratory is discussed using fabric, strain and paleostress analyses, for the case of Oligocene Boom Clay (Belgium). Non-dilatant ductile and dilatant brittle structures develop successively in the stress path of the deforming mud, which remains close to its critical stress state due to its low strength. The transition between the failure modes depends on the mean effective stress, the water content, the amount of strain and the burial-uplift history. The specific stress path initially follows a K_0 path that is left when differential stress increases, due to both uplift and compaction-induced endogenous forces, reflected by a decrease in effective confining pressure prior to failure, and far-field tectonic forces, reflected by the distinct and regular orientation of fractures. The related deformation is ductile, causing distributed micro-shear bands, up to the dilatancy boundary, beyond which extensional fractures develop.

Keywords: Soft-sediment deformation; Brittle–ductile transition; Microtectonics; Critical state mechanics; Microfabric

1. Introduction

The micromechanics of fracturing and the development of dilatant fracture permeability have been extensively studied for crystalline and siliciclastic cemented rocks (Rutter and Hadizadeh, 1991; Lockner et al., 1992; Menéndez et al., 1996; Wong et al., 1997; Ngwenya et al., 2000; Rogers, 2003). They have received much less attention in uncemented or poorly cemented sediments (Jones and Addis, 1986; Agar et al., 1988; Arch et al., 1988; Mertens et al., 2003; Dehandschutter et al., 2004). However, *mud*, referring to a weakly consolidated, highly porous and water-rich argillaceous sediment mainly composed of clay- and silt-sized particles containing high quantities (>2/3) of clay minerals (Blatt et al., 1980), and *mudstones*, their compacted and cemented equivalent, often display intense fracturing that develops in the early stages of basin evolution when the sediments are still highly porous, water-rich and uncemented (Maltman, 1984; Aplin et al., 1999). Fracture development in mud and mudstone can have important consequences for fluid-flow changes (fracture permeability) and mechanical strength of the rock body, both key parameters determining the hydrocarbon cap-rock capacity of mud and its barrier properties with regard to its use as (surface and underground) host formation for waste repositories. In cases of strain softening, fractures can provide major planes of weakness facilitating shear and reducing the bulk rock strength. Consolidated mud(stone) has a very low hydraulic conductivity and is virtually impermeable, but the occurrence of brittle, dilatant fractures can provide pathways for fluid flow, increasing the permeability by several orders of magnitude (Sibson, 1981). Fracture porosity and related fluid flow will develop

* Corresponding author. Currently at: International Bureau for Environmental Studies, Ortar Depauwstraat 49, 3080 Tervuren, Belgium. Tel.: +32 2 784 30 63; fax: +32 2 306 48 53.
E-mail address: bodehand@ibes.be (B. Dehandschutter).

0191-8141/$ - see front matter © 2005 Elsevier Ltd. All rights reserved.
doi:10.1016/j.jsg.2004.08.014

only in the case of dilatancy, associated with volumetric strain under differential stress (Ingram and Urai, 1999). In other cases, permeability inside the fracture zone will be decreased (Jones and Addis, 1985; Arch and Maltman, 1990). Additionally, fractures in mud can greatly increase the surface area susceptible to weathering and hence strongly affect the mud's engineering properties.

Although striated and polished slip surfaces (slickensides) have long been observed in many naturally deformed argillaceous sediments (Skempton, 1964; Faas and Crockett, 1983), studies of the geomechanical and micro-tectonic (fabric) characteristics of such slickensides occurring in natural exposed mud deposits have received only limited attention in geological and engineering literature. On the other hand, many experimental studies report the development of shear bands in mud(stone) during deformation experiments (Morgenstern and Tchalenko, 1967; Tchalenko, 1968; van den Berg, 1987; Arch et al., 1988). Shear fabric observed in mudstone from ODP boreholes have been described by backscattered scanning electron microscope (SEM) imagery (Agar et al., 1988; Takizawa and Ogawa, 1999). The change of rock strength by fracture development has been studied in the context of hydrocarbon exploration, where discontinuities in cap-rocks can cause hydrocarbon leakage and stability problems (Ingram and Urai, 1999). This study contributes to the understanding of brittle to ductile transitional behaviour of mud deforming in near-surface conditions, by providing a detailed (micro-) morphological and (micro-)structural description of outcropping argillaceous sediments.

The Oligocene Boom Clay is a thick argillaceous sequence present in much of the North Sea basin and outcropping in northern Belgium. It has been selected as a possible host rock for deep and long-term (geological) radioactive waste disposal and in this context extensively studied (ONDRAF/NIRAS, 2001). Underground research facility excavation in the Boom Clay at 225 m depth revealed intense fracturing of the mud (Dehandschutter et al., 2002, 2004; EURIDICE, 2003; Mertens et al., 2004), imposing questions on the characteristics (permeability) and origin (formation mechanism) of the fractures both at depth and in clay pits at the surface. Recognition of fractured Oligocene mud in the North Sea (Clausen et al., 1999) and equivalent Tertiary muds (Henriet et al., 1991; Cartwright and Lonergan, 1996) further encouraged a detailed study of fracture characteristics and fracturing mechanisms in mud.

2. Methodology

Detailed field mapping has been used to statistically analyse the orientation of the various structures (faults and joints), in relation to their environment (stratigraphic level and composition). Kinematic and dynamic analysis allowed the assessment of local and regional deformational regimes (shortening and extension directions) at the time of the fracture formation as well as paleostress reconstructions, obtained using classical methods of kinematic data inversion (Hancock, 1985; Angelier, 1994; Dunne and Hancock, 1994). These methods consist of determining the best fitting reduced paleostress tensor for a given set of geological kinematic data. The paleostress tensor describes the orientations of the principal compressive stress axes (minimum (σ_3), intermediate (σ_2) and maximum (σ_1)) and the ratio of principal compressive stress difference R, determining the shape of the stress ellipsoid.

Analysis of the mud's microfabric has been carried out using SEM imagery. Sample preparation was performed by slow air drying and subsequent controlled cracking along pre-cut ditches parallel to the movement direction and perpendicular to the bedding (in the case of slip-planes) or perpendicular to a fracture surface and perpendicular to the bedding (in the case of joints). A detailed description of microfabric sample preparation and analysis methodology can be found in Dehandschutter et al. (2004).

The above techniques are combined to get a better insight into the deformation of argillaceous sediments. Comparison of geometric, kinematic, dynamic and microfabric characteristics of the different fracture types, their cross-cutting relations and their relations to the mud's geotechnical characteristics and geological history are used to develop a model explaining the rheological properties of argillaceous sediments and predict their deformation behaviour during their geological evolution.

3. Geological settings

3.1. Stratigraphy

The Boom Clay (Rupelian, Oligocene) crops out along an intensely brick-mined cuesta-front in northern Belgium (Fig. 1), and extends in sub-crop over large parts of the North Sea basin (Vandenberghe, 1978). It dips gently ($\sim 2^\circ$) towards the northeast and increases in thickness from a few decametres in the outcrop area to more then 150 m in the deeper parts of the basin. The Oligocene deposits are part of the Cretaceous–Cenozoic sedimentary cover onlapping the Paleozoic London–Brabant Massif basement (Fig. 1). The sediments are detrital marine deposits composed of rhythmically alternating clay-rich and silt-rich beds resulting in a typical gray-tone banding (Fig. 2). Individual bed thickness ranges from metre-scale at the base to centimetre-scale in the higher parts of the section. Based on cyclic variations in granulometry, organic matter content and carbonate content, the Boom Clay is divided into three members (Vandenberghe, 1978; Vandenberghe et al., 1998; Fig. 2). The cyclicity in the Boom Clay has been attributed to relative sea level cycles (Laenen, 1999) and climatic changes (Van Echelpoel and Weedon, 1990; Vandenberghe et al., 1997). On several stratigraphic levels, carbonate-rich lime bands of decimetre-scale thickness occur, inside which

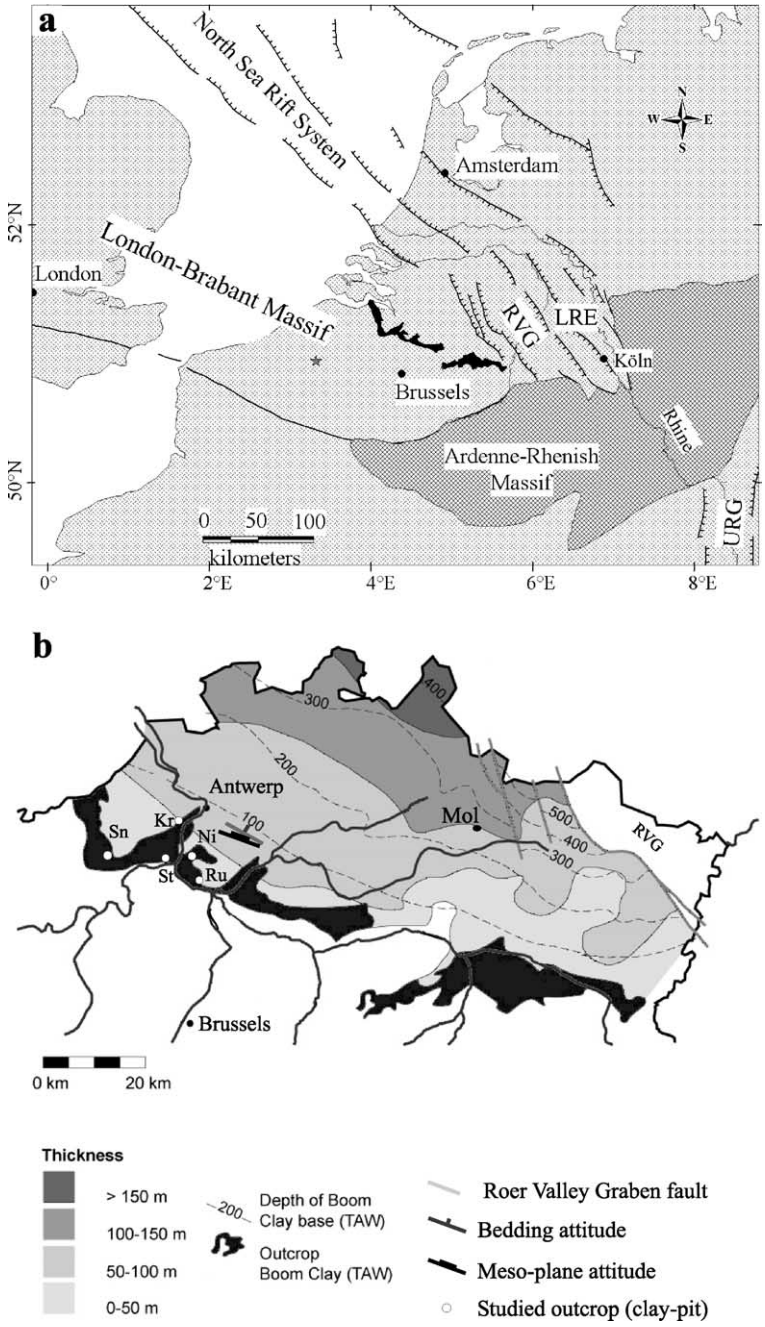

Fig. 1. (a) Structural sketch of northwestern Europe with the outcrop area of the Boom Clay (black area). LRE: Lower Rhine Embayment; RVG: Roer Valley Graben; URG: Upper Rhine Graben. Grey star indicates outcrop of Ypres Clay. (b) Structure contours and isopachs of the Boom Clay (after ONDRAF/NIRAS, 2001). Studied outcrops: Kr: Kruibeke; Sn: Sint-Niklaas; St: Steendorp; Ni: Niel; Ru: Rumst.

diagenetic oval calcite-concretions (septaria) have formed (Vandenberghe, 1978; De Craen et al., 1999). They are well expressed in the field and numbered S05 to S80 (Fig. 2). The decimetre-scale banding in the Boom Clay allows stratigraphic control of the position of the fractures observed in the different studied clay pits. The upper part of the Boom Clay has been eroded in the outcrop zone and is only found in cores in northern Belgium. This Chattian erosion event reflects the Late Oligocene uplift of the London–Brabant and Ardenne–Rhenish massifs (Fig. 1), before the deposition of Neogene marine sands (Berchem Formation) unconformably onlapping the Boom Clay in the outcrop area (Vandenberghe et al., 1997).

3.2. Physical and geotechnical characteristics

The Boom Clay is an unlithified mud, mainly composed of kaolinite and illite with minor amounts of smectite and chlorite (Vandenberghe, 1978; Laenen, 1999). In its outcropping part (clay pits), it has an average water content

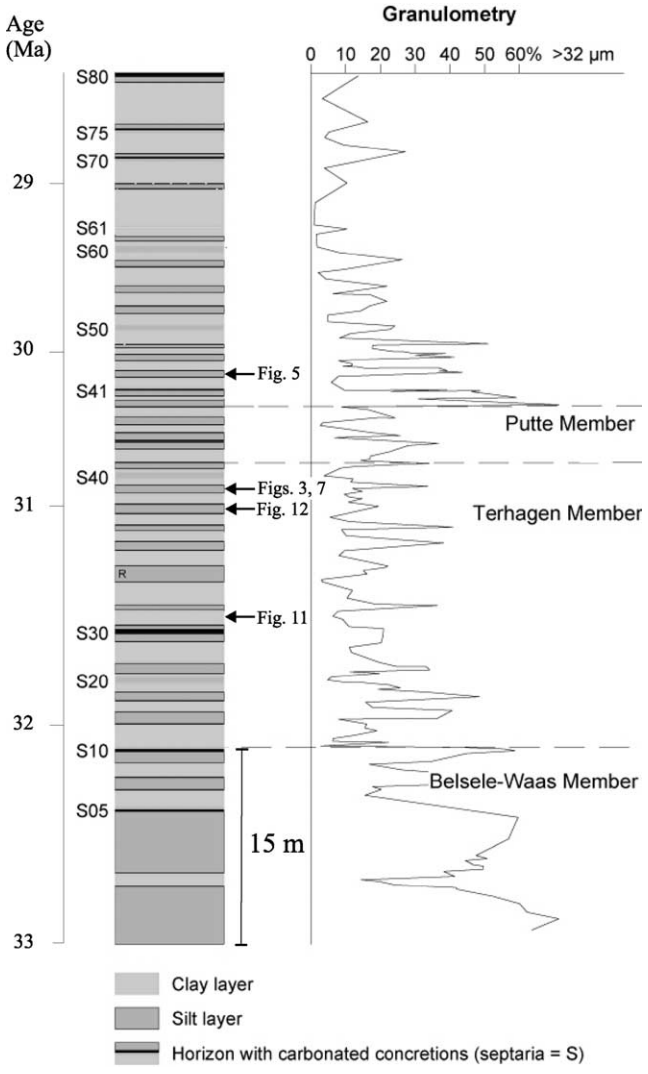

Fig. 2. Stratigraphic section of the lower (outcropping) part of the Boom Clay (after Vandenberghe et al., 1998; ONDRAF/NIRAS, 2001). S05 to S80 refer to septaria levels. Black arrows indicate the stratigraphic level of other figures and samples.

of ~25%, and a physical porosity of ~35%. Mercury intrusion experiments indicated a connected porosity varying between 0.25 and 0.28 (Dehandschutter et al., 2004) and an entrance pore diameter around 200 nm (Al-Mukhtar et al., 1996; Romero et al., 1999; Dehandschutter et al., 2004). The average soil properties of Boom Clay are presented in Table 1. Unconsolidated undrained triaxial tests estimate the undrained shear strength for Boom Clay at outcrop to be around 175 kPa, classifying it as a stiff to very stiff clay (Schittekat et al., 1983). Estimates of the OCR range from 1 to 3 (Schittekat et al., 1983; Mertens et al., 2003). Estimates of the effective elastic modulus range from 110 MPa (derived from the shear modulus; Schittekat et al., 1983), through 200 MPa (Horseman et al., 1987) to 300 MPa (Labiouse and Bernier, 1997), depending on the water content and sample depth. Estimates based on geophysical wire-line data give undrained values for the Young modulus of 1600–2000 MPa (ONDRAF/NIRAS, 2001), and sonic logs on drained core samples give even 5000 MPa (own unpublished results). For saturated outcropping Boom Clay, discussed in the present study, 150–200 MPa is taken as a value for the undrained Young modulus.

3.3. Geodynamic settings

The Oligocene Boom Clay is located at the southwestern border of the North Sea basin. Deformation of Cretaceous and Tertiary deposits in France, England and Belgium indicates that northwestern Europe evolved in a normal faulting regime with a dominant E–W extension direction during much of the Paleogene (Bergerat and Vandycke, 1994; Vandycke, 2002). After early Eocene extension in the North Atlantic and North Sea, the North Sea rift system (Fig. 1) became tectonically quiescent and the later evolution of the North Sea basin was mainly governed by thermal relaxation (and subsidence) of the lithosphere, its loading by sediments and far-field responses to Rhine Graben activity and Alpine forces. The thickness of Eocene and younger deposits (up to 3.5 km) increases towards the centre of the basin, parallel to the NNW-trending Central Graben and Viking Graben axes. At the onset of the Oligocene, regional subsidence resulted in the broadening of the North Sea Basin. The Early Oligocene (Rupelian) sedimentation was terminated by Late Oligocene (Chattian) erosion, caused by the uplift in the south of the Ardenne–Rhenish and London–Brabant massifs (Letsch and Sissingh, 1983).

The strongest Neogene deformation in NW Europe is represented by a normal faulting regime with NE–SW extension direction causing NW–SE-trending joints and normal faults (Vandycke, 2002). Intense deformation of this kind has also been reported in England and attributed to a Miocene tectonic phase (Bevan and Hancock, 1986).

The currently most active region in NW Europe is the Roer Valley Graben at the southwestern border of the Lower Rhine Embayment (Fig. 1; Dirkzwager et al., 2000). Here, the main tectonic subsidence started in the Late Oligocene due to border fault activity and has been peaking since the Miocene (Sintubin et al., 2002; Michon et al., 2003).

Morphological studies (Camelbeeck and Meghraoui, 1998; Meghraoui et al., 2000), show that the active tectonics of NW Europe is dominated by NE–SW extension along NW–SE-trending normal faults. In situ stress measurements indicate that the horizontal component of maximum principal compressive stress (SH_{max}) trends NW–SE, and the horizontal component of minimum principal compressive stress (SH_{min}) trends NE–SW (Müller et al., 1992), suggesting the prevailing nature of this regime. In NE Belgium, the current extensional dynamics of the Roer Valley Graben has been active since the Oligocene, with varying extension from N–S to NE–SW (Camelbeeck and Meghraoui, 1996; Paulissen, 1997).

Table 1
Average soil and geotechnical properties of Boom Clay near the surface, compiled from Al-Mukhtar et al. (1996) and Schittekat et al. (1983)

Soil properties	
In situ density	1900 kg m^{-3}
Water content	25–30%
Porosity (total and connected)	0.35 and 0.28
Liquid limit	70%
Plastic limit	25%
Plasticity index	45%
Cohesion	175–300 kPa
Angle of internal friction ϕ	18°
Poisson ratio ν	0.4
Elastic modulus E	110–300 MPa (?)
Shear modulus G	40 MPa
Undrained shear strength	170–200 kPa
Unconfined compressive strength	2.2 MPa?
Tensile strength	100 kPa (?)
K_0	0.7 (?)
OCR	?

4. Fracture characteristics

4.1. Faulting and jointing

4.1.1. Meso-planes at the Kruibeke fault zone

In the clay pit of Kruibeke (Kr in Fig. 1), a series of sub-parallel normal faults composes a fault zone several metres wide. The fault zone comprises at least five individual sub-parallel normal faults, spaced at about 5 m each. Each individual fault is around 5 m high. The maximal net displacement along an individual fault is about 1 m (Fig. 3a). Each normal fault, when examined in detail, turns out to be composed of several sub-parallel centimetre-scale slickensides (hereafter called *meso-planes*) composing a secondary fault zone, varying in width from zero (only one slip surface) to several decimetres (Fig. 3b). The orientation of most of the meso-planes is parallel to the macro-scale fault they compose, although locally antithetic slickensides occur inside the fault zone (Fig. 4). In some cases internal features such as septaria nodules are rotated within the fault zone (Fig. 3c and d). Nearly all meso-planes inside the fault zone show normal displacements (Fig. 4). The whole of the slickenside orientations fits in a single deformation regime with a northeasterly oriented extensional direction, associated with the northeasterly normal offset of the hanging-wall fragments (Fig. 4). The average strike-trend azimuth of the fault zone is 120° and it dips on average 50° to the northeast (Fig. 4).

4.1.2. Micro-planes

A second fracture type comprises regionally recognized centimetre-scale slickensides, hereafter called *micro-planes*. Planes of this type are present in all investigated clay-pits. They are smaller in size (order of magnitude 3–6 cm) than the meso-planes. They occur randomly distributed over the outcropping parts of the Boom Clay, although more abundantly in the clay-rich layers, where the

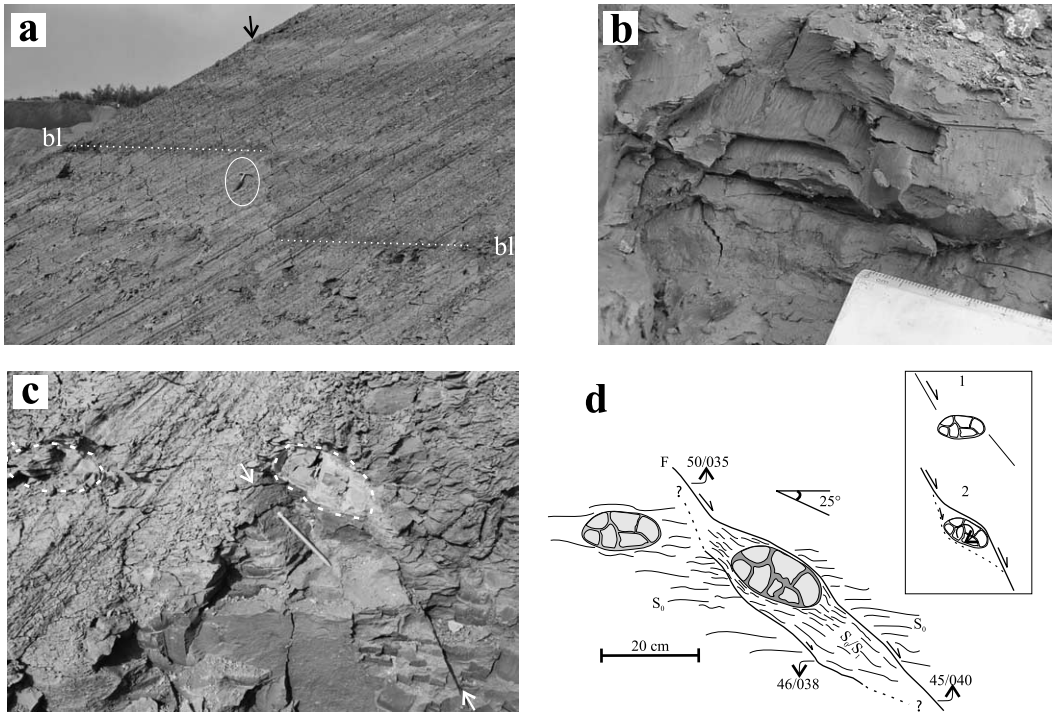

Fig. 3. Photographs of a fault in the Kruibeke fault zone (Kr in Fig. 1). (a) Apparent displacement of the black layer (bl, dashed white line). Hammer for scale. Fault trace indicated by black arrow. (b) Detail of the segmented nature of the composing meso-planes. (c) Close-up in the fault with composing strands (white arrows), and rotated septaria (white traces) between two strands. (d) Sketch of the differential displacement along individual strands causing internal rotation (inset).

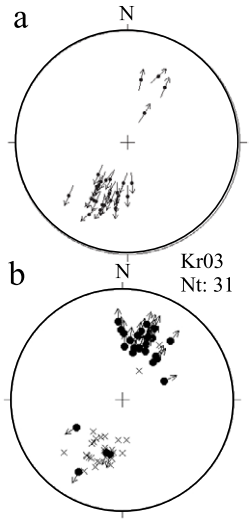

Fig. 4. (a) Stereographic projection (equal-area, lower-hemisphere) of 31 poles (Nt) with tangent lineations (Hoeppener, 1955) of individual fault-strands composing the meso-scale fault zone at Kruibeke (Kr in Fig. 1). (b) Separate plot of poles to fault planes (crosses) and slickenlines (circles with sense indicators).

spacing can reach up to about 10 cm. Displacement is predominantly dip-slip with minor pitch variations of about 15°. Their surface is generally smooth (shiny and polished) and striated, with linear slickenlines oriented parallel, or sometimes in conical distribution (Fig. 5). Although the striae on the planes indicate shear displacement, fault throw could not be determined and must be minor (see Section 4.3). Based on observations of secondary structures (Riedel shear, releasing bands, etc.), the slip has been determined to be dominantly normal (hanging wall down). Criteria used to determine the shear sense are described by Angelier (1994) and Dunne and Hancock (1994).

The slickensides occur both in freshly excavated quarry fronts and in weathered zones of old excavation fronts, and have no correlation with the excavation wall orientation. This rules out their origin being induced by artificial, post-excavation alteration (shrinkage, desiccation–accommodation).

A detailed statistical analysis indicates clustering of the micro-planes (Fig. 6). Over the whole outcrop region, the dominant strike of the micro-plane slickensides is clearly 120° (or between 110 and 130°). A secondary dominant strike is around 040°. The dip of the slickensides is dominantly around 50–60°, although very flat and very steep planes occur occasionally (Fig. 6).

4.1.3. Joints

Mode I vertical fractures are abundant in the whole section of all outcropping clay-pit faces. They occur as regular sets and become particularly pronounced after weathering (Fig. 7). They are very persistent in trend (strike) and always sub-vertical. A previous study (Mertens et al., 2003) has already shown that they are independent from excavation front orientation and have to be considered natural and of regional importance. The joint spacing ranges from 1 m in some clay-rich layers to several metres in the silt-rich layers. Statistically, the mean orientation of the joints shows an average strike of 130° (J_1 in Figs. 7 and 8) and a

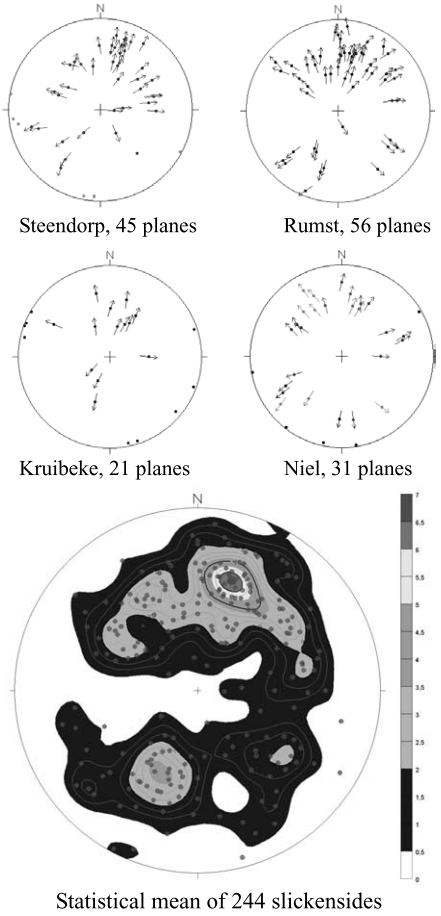

Fig. 6. Examples of equal-area lower-hemisphere stereographic projections of slickensides (poles and tangent lineations) at individual clay-pits (locations in Fig. 1), and statistics of all 244 measured planes (stereographic projection and frequency distribution) indicating trend anisotropy.

Fig. 5. Typical micro-plane slickensides occurring in the outcropping Boom Clay. Pencil-top in the lower middle of the photograph is about 1 cm big.

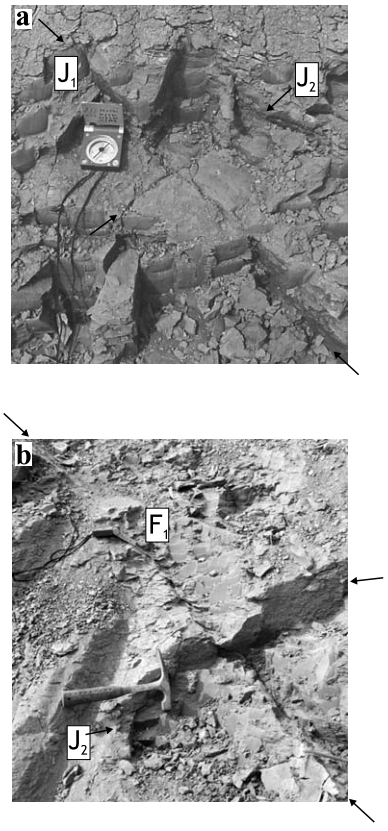

Fig. 7. Photographs showing the expression of sub-vertical jointing in Boom Clay outcrops. (a) Orthogonal principal joint sets J_1 and J_2. (b) J_2 plane (near hammer) cutting a meso-plane fault strand (from pencil to compass), indicating that the formation of J_2 postdates the faulting phase.

smaller population striking 30° (J_2 in Figs. 7 and 8). Notice the close correlation in trend between the joints (Fig. 8), the micro-planes (Fig. 6) and the meso-planes (Fig. 4).

The two dominant joint trends are recognized all over the outcrop area (more than 100 km in the E–W direction; Fig. 1), and also have been observed in Eocene Ypresian Clay, outcropping 100 km to the west (grey star in Fig. 1a). They can be therefore considered of regional importance. The two main joint sets are mutually (sub-)perpendicular, a situation that seems to be common in many jointed rock formations (Caputo, 1995). Using cross-cutting geometries (Hancock, 1985) to establish a relative chronology for the

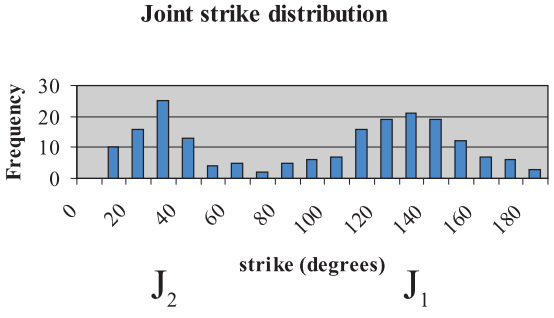

Fig. 8. Frequency distribution of joint strike (all 196 points). Main joint sets strikes around N130°E (J_1) and N30°E (J_2).

two orthogonal joint sets, a grid-lock pattern (Hancock et al., 1987) of both joint sets has been revealed, suggesting that both sets are coeval.

4.2. Stress evolution

The paleostress results derived from fault-slip analysis of meso- and micro-planes (Fig. 9) show that all the observed movements developed in a normal faulting regime (sensu Anderson, 1951; Table 2). Stereographic projection of the principal compressive stress axes and the average movement plane organized per measurement station reveal the consistency of the average fracture-strike and movement directions and consequently of the principal paleostress axes orientations (Fig. 10). The average extension direction (SH_{min} and σ_3) trends 032°, indicating a nearly NE–SW extension direction. The average SH_{max} trends 122°, which is nearly NW–SE (Table 2).

The parameter R (ratio of principal compressive stress

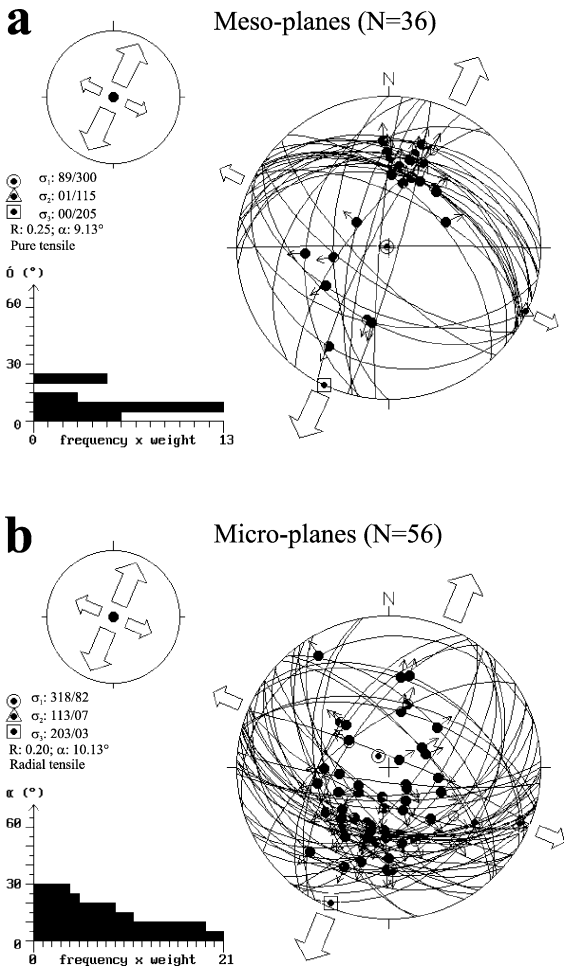

Fig. 9. Examples of paleostress calculations. Equal-area, lower-hemisphere projections of fault planes (great circles), striae (small arrows) and principal compressive paleostress axes. Large outlined arrows and squares indicate SH_{max} direction (σ_2), small outlined arrows and triangles indicate the SH_{min} direction (σ_3), from fault-slip data of meso-planes (a) and micro-planes (b). Symbols explained in Table 2.

Table 2
Paleostress reconstruction and statistics

Site	Latitude	Longitude	Clay-pit description	n	nt	σ_1	σ_2	σ_3	R	α	Q	R'
Kr01	51.21	4.33	Kruibeke, w.f., me.p.	39	37	88/339	00/075	02/165	0.30	12.12	B	0.30
Kr03	51.21	4.33	Kruibeke, w.f., me.p.	35	43	83/299	07/133	02/043	0.25	9.42	A	0.25
Kr08	51.21	4.33	Kruibeke, f.f., mi.p.	13	16	85/310	05/112	02/202	0.18	7.63	A	0.18
Ru01	51.09	4.40	Rumst, w.f., mi.p.	33	46	87/256	02/120	03/030	0.20	11.15	B	0.20
Ru02	51.09	4.40	Rumst, f.f., mi.p.	34	39	82/318	07/113	05/203	0.19	7.37	A	0.19
St01	51.14	4.27	Steendorp, w.f., mi.p.	37	48	79/019	00/288	11/198	0.16	7.74	B	0.16
Sn01	51.13	4.12	Sint-Niklaas, f.f., mi.p.	43	52	85/121	04/313	01/223	0.23	7.8	B	0.23
Ni01	51.16	4.35	Niel, f.f., mi.p.	31	31	88/125	01/310	05/225	0.23	10.2	B	0.23
Mean for all clay-pits				265	312	85/258	03/122	04/032	0.21	9.17		0.25

Coordinates are given in decimal degrees; w.f.: weathered front; f.f.: fresh front; me.p.: meso-plane; mi.p.: micro-plane. n is the number of geological structures used to calculate the reduced paleostress tensor. nt is the total number of measured kinematic structures. σ_1,σ_2 and σ_3 are, respectively, the maximal, intermediate and minimal compression directions of the stress ellipsoid (dip/dip direction). $R=(\sigma_2-\sigma_3)/(\sigma_1-\sigma_3)$ is the ratio of principal compressive stress differences. It is indicative of the state of stress corresponding to a tensor. α describes the mean deviation between theoretical and observed fault movement. It is a measure of the accuracy of the calculated tensors. Q is quality of the calculated tensor, taking into account n, nt and α. R' is the stress type index (Delvaux et al., 1997). It varies gradually between 0 (radial extension) and 3 (radial compression). For $0.25<R'<0.75$ the regime is pure tensile; for $0.75<R'<1.25$ it is transtension; for $1.25<R'<1.75$ it is pure strike-slip; for $1.75<R'<2.25$ it is transpression, and for $2.25<R'<2.75$ the stress regime is pure compressional.

differences) describes the shape of the stress ellipsoid by giving the relative magnitude of σ_2 between σ_3 and σ_1. Low values of R indicate that the magnitude of σ_2 is close to σ_3, whereas high values of R mean that the magnitude of σ_2 is close to σ_1. In the present study, where σ_2 and σ_3 are both horizontal, higher R-values reveal a higher horizontal stress anisotropy resulting in a stronger preferential orientation of the fractures. The results show clearly that meso-plane related structures (Kr01 and Kr03 in Table 2 and Fig. 9a) have distinctly larger R values than the micro-plane related

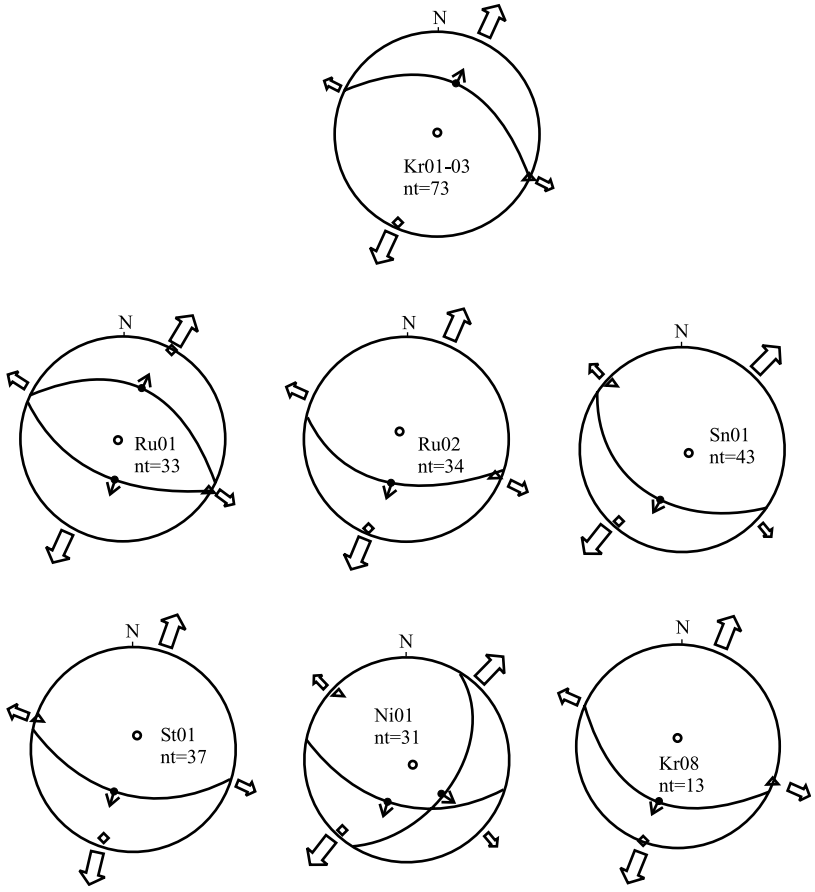

Fig. 10. Stereographic projections of the principal compressive paleostress axes derived from kinematic analysis of fault-slip data from meso-planes (Kr01–03) and micro-planes (rest), organized per station (see Table 2 and Fig. 1). The average movement plane(s) and striae directions are indicated for each station. Large outlined arrows and squares indicate SH_{max} direction (σ_2), small outlined arrows triangles indicate the SH_{min} direction (σ_3).

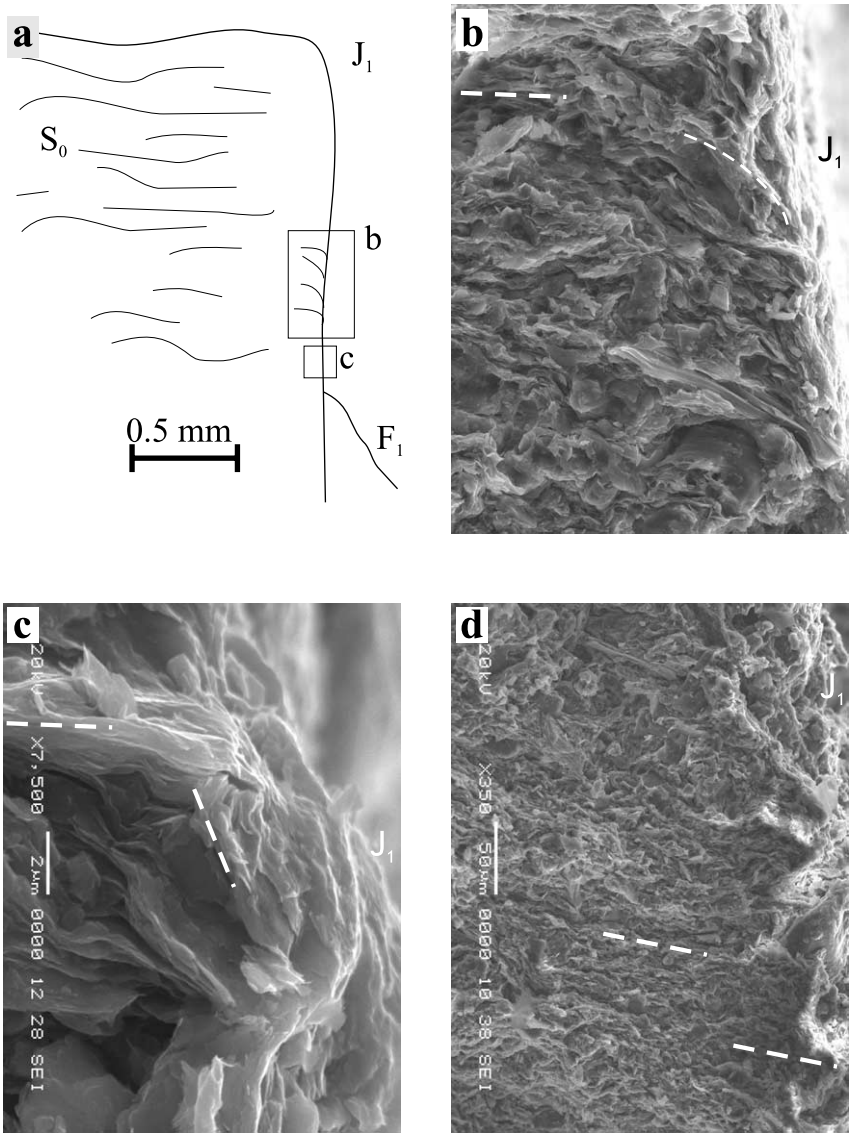

Fig. 11. SEM images of a sub-vertical 130°-striking joint (J_1). (a) Outcrop sketch of sampled J_1 with bedding S_0 and nearby dip-slip slickenside F_1. (b) Ductile shear bands near the joint surface (white stippled line indicates bedding). (c) Close view of reoriented bedding. (d) Example of joint surface without shear (pure mode I failure). This structure occurs about 10 cm above (b).

structures (Ru, St, Sn and Ni in Table 2 and Fig. 9b) and thus formed under more anisotropic stress conditions. The faulting regime is described by the parameter R' (Table 2). For the Kruibeke fault zone the regime is pure extensional faulting, shown by R'-values above 0.25 (Fig. 9a), whereas the micro-planes tend more to a radial extensional faulting regime (Fig. 9b), reflected by their R'-values below 0.25 (Delvaux et al., 1997; Dehandschutter, 2001). The slip deviation α (discrepancy between observed and calculated slip direction) remains relatively low (9.2° on average) and the quality index Q of the calculated tensors is good, indicating a good reliability of the results (Table 2).

4.3. Microfabric of fractures in the boom clay

A total of 15 samples of meso-planes, micro-planes and joints have been investigated using SEM microscopy. The well-expressed sub-horizontal bedding anisotropy is used as a reference plane highlighting fabric changes such as clay-particle rotation, translation or extension related to fractures.

Several vertical joint walls display sub-horizontal bedding, without noticeable changes of bedding orientation in the vicinity of the joint plane (Fig. 11d). This regularity, however, cannot be generalized. Some of the joints show a distinctive component of shear displacements in the vicinity of the fracture surface (Fig. 11b and c). In the case presented in Fig. 11, the sample was taken close to a micro-scale slickenside trending parallel to the main joint, but dipping much less steeply, at around 40° (Fig. 11a). The apparent (micrometric) displacement observed in the joint wall (Fig. 11b and c) is synthetic with the normal offset along

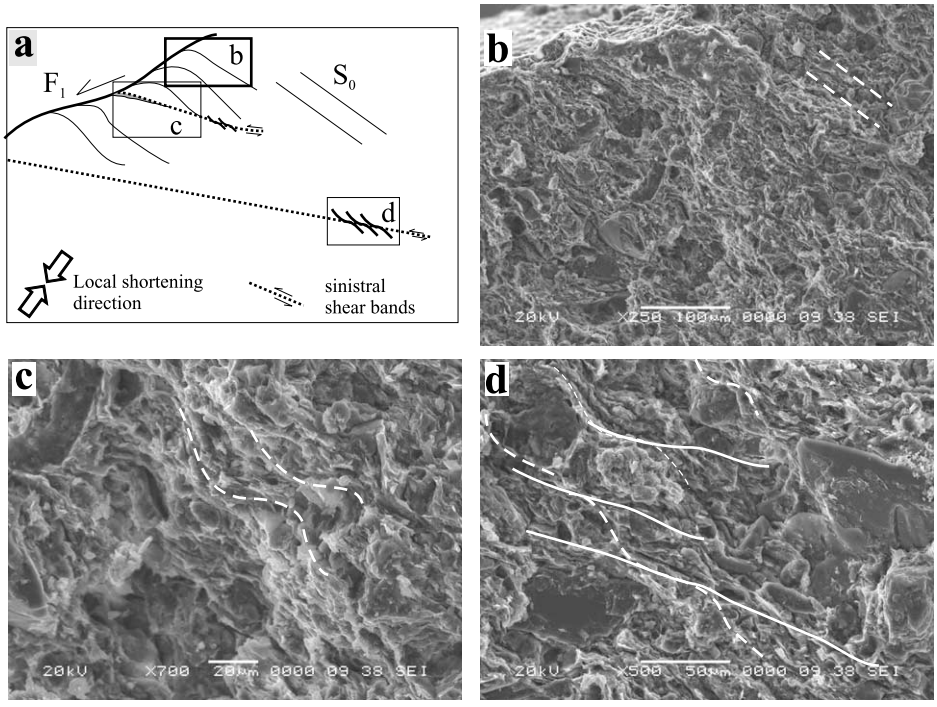

Fig. 12. Slickensided fracture F_1 related to J_1 and showing particle rotation (b), and sinistral synthetic shear band development (c and d). S_0: bedding (indicated by white stippled lines). White lines on (d) indicate shear bands.

the slickenside (F_1 in Fig. 11a). Often, secondary shear zones develop in the vicinity of a J_1 fracture at a small angle to it. Those shear zones are local zones in which the clay particles are aligned by grain-boundary sliding and particle reorientation. The particle alignment occurs at the expense of the porosity between the clay particles, and hence results in local compacted zones.

The microfabric in the vicinity of several slickensides (micro-planes) also shows secondary shear zones with particle alignment (Fig. 12). Close to the slickenside surface, clay particles are rotated in the movement direction by shear-induced drag (Fig. 12b). Inside the footwall, synthetic sinistral shear bands develop (Fig. 12c and d). Several zones of strongly localised deformation in anastomosing shear bands have been observed in nearly all samples (Figs. 11 and 12).

Local zones of dilatancy are also observed in several samples. The dilatancy zones often compose en-échelon tension gashes, or secondary Riedel shears and dilatant reactivated bedding planes (Dehandschutter et al., 2004).

5. Mechanical behaviour of argillaceous sediments

5.1. The brittle–ductile transition

Considering the deformation of weak argillaceous sediments, the concepts of brittle and ductile behaviour and deformation have specific connotations. Unlike for hard-rock geology, brittle and ductile processes in the low-temperature regime are regarded essentially as being temperature independent (Rutter and Hadizadeh, 1991). Thermally controlled processes such as diffusive mass transfer and intercrystalline plasticity are therefore not considered. For clarity, criteria discerning both rheological responses are provided (Table 3). In a phenomenological sense, ductile behaviour (sometimes called cataclastic flow (Menéndez et al., 1996; Wong et al., 1997; Table 3) indicates that the material can sustain large, continued, inelastic deformation during plastic hardening. Brittle behaviour indicates the abrupt failure of a basically elastic material at well-defined peak strength with subsequent loss of cohesion and strong softening. Fluid flow through fracture permeability, however, can only be induced when the material is brittle and dilates, strain is large enough and the dilatant fractures are connected (Sibson, 2000).

The microscopic processes responsible for both deformation modes are still poorly understood, especially for ductile behaviour (Wood, 1990; Pouya et al., 1998; Al-Shayea, 2001). Brittle failure mechanisms include grain crushing, abrasion, intergranular sliding, grain reorientation and the growth of micro-cracks. However, the mechanisms for ductile deformation, on a sub-microscopic level, might very well be the same as those of brittle deformation (Rutter, 1986; Menéndez et al., 1996; Wong et al., 1997).

One and the same material can yield in different deformation modes under varying confining pressure. When sheared at high confining pressure, the mudrock behaves in a ductile manner, whereas at low confining pressure the same rock deforms in a brittle manner (Petley,

Table 3
Brittle versus ductile behaviour in the low-temperature regime

	Brittle behaviour	Ductile behaviour
Permanent strain before failure	<3%	>5%
Strain hardening	No	Yes
Loss of cohesion	Yes	No
Stress drop at failure	Yes	No
Strain	Localised	Diffuse
Micro-cracking	Localised	Distributed
Dilatancy	Strong	Absent or weak
Peak strength	Strongly defined	Poorly defined
Stiffness	High	Low
Alternative address	'Dry side' deformation	Cataclastic flow, 'wet side' deformation

1999; Fig. 14). The water content (Al-Shayea, 2001), amount of strain (pre-peak shearing; Mandl, 1999), over consolidation ratio (OCR; Jones and Addis, 1985; Burland et al., 1996; Ingram and Urai, 1999) and strain rate (Arch et al., 1988) of mud also strongly influences its deformation mode (brittle or ductile; Fig. 14).

5.2. Critical state mechanics

Critical state mechanics describes the deformation of uncemented sediments accounting for void ratio changes (compaction, dilatancy), confining pressure changes (burial/uplift cycles) and differential stress (Fig. 13). Several yield envelopes confine elastic deformation between the normal consolidation line (NC, in the absence of differential stress), K_0-line (ratio of horizontal effective stress/vertical effective stress) and the critical state line (CSL), determining the transition from elastic to compacting ductile or dilatant brittle behaviour (Fig. 13). During burial of weak argillaceous sediments, horizontal stress remains close to the vertical load resulting in a fairly high K_0 value (0.6 to 1). At a certain critical void-ratio and differential stress, the sediment will yield (change from elastic to elasto-plastic behaviour), and deform along a hardening path (ductile) towards its critical state, at which large strain can be realized with minor stress changes. Alternatively, the sediment can deform by dilatancy and strong stress drop (brittle failure) towards residual stress level (Jones and Addis, 1986; Wood, 1990). The CSL (Fig. 13a) defines the maximum stress levels a sediment volume can attain before dilatancy (brittle failure) in p', q and e-space.

The 'dry side' and 'wet side' deformation (Fig. 13b) is followed by heavily overconsolidated and weakly to normally consolidated argillaceous sediments, respectively. Alternatively stated, overconsolidated sediments (with an overconsolidation ratio $p'_{max}/p'_{actual}OCR > 1$) generally deform in brittle mode and undergo dilation, whereas normally consolidated sediments, lacking strong uplift, undergo ductile (and compacting) deformation (Fig. 14).

6. Discussion

6.1. Fabric and micro-tectonic relations

6.1.1. Slickensides and micro-planes

Slickensides can form under a wide variety of geological and mechanical conditions. *Pedogenic slickensides* are related to their clear near-surface, hydro-gravitational origin

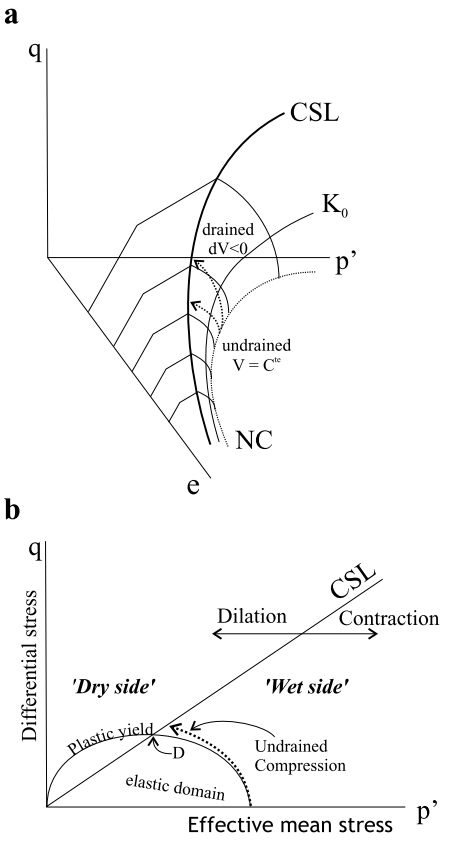

Fig. 13. Critical state principles. (a) Critical state line (CSL), normal consolidation line (NC), K_0 line in mean effective stress (p')—deviatoric stress, (q)—void ratio, (e)—space. Typical stress paths for drained and undrained experimentally deformed (triaxial compression) sediments. (b) Elliptical plastic yield surface in p'–q space delimiting 'wet-side' (ductile, cataclastic flow) and 'dry side' (brittle, dilatant) deformation.

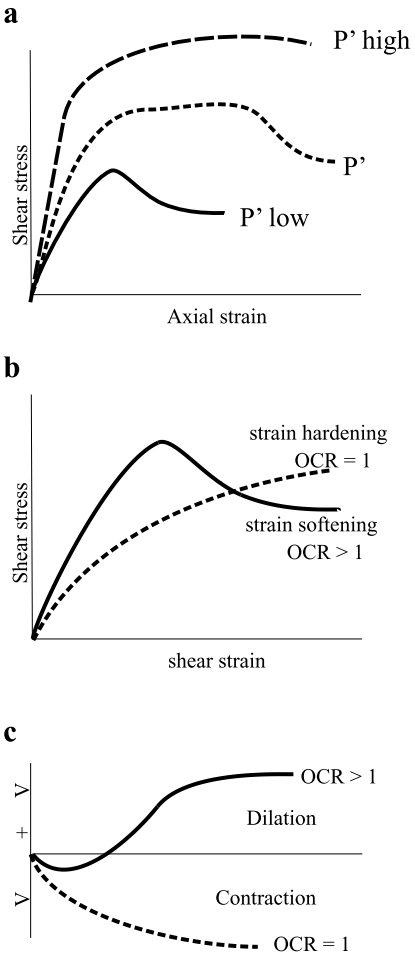

Fig. 14. (a) Brittle, transitional and ductile behaviour of mudstone with increasing confining pressure, in shear stress (τ)—axial strain (ε)—space. (b) Influences of the OCR on the brittle–ductile behaviour of mudstone deformation. (c) Variable volume changes in function of OCR.

in wetting and drying soil (Gray and Nickelsen, 1989) and are therefore distinguished from *hydroplastic slickensides*, which can have either a tectonic or a *sedimentary* origin (Petit and Laville, 1987). Hydroplastic behaviour is common in weak, porous and uncemented sediments and is situated in the rheologically transitional field between brittle and ductile deformation (Petit and Laville, 1987). *Brittle slickensides* result from shear failure in brittle rock and form on a discrete fault plane by polishing of fault gauge, by drag of wear material or by the syn-kinematic growth of minerals during fault slip (Means, 1987). There are several criteria to distinguish brittle from hydroplastic deformation, based on the difference between brittle and hydroplastic rheology (Table 4).

The small-scale slickensides observed all over the outcrop area of the Boom Clay have several regular characteristics. Except for some curviplanar, conically striated, flat-lying shear planes, most slickensides are planar and dip moderately to steeply (Fig. 6). They mostly have planar dip-slip striae (rarely fan-shaped) and are considered to have formed under vertical shortening and vertical maximal principal compressive stress (σ_1). With these characteristics, they can hardly be classified as pedogenic or sedimentary hydroplastic slickensides that would result from water expulsion during burial history (Table 4; Guiraud and Séguret, 1987). Additionally, unlike pedogenic and sedimentary hydroplastic slickensides, the described structures have a tendency to cluster around specific trend-directions (Fig. 6), indicating anisotropic horizontal stress and tectonic control. The microfabric related to the micro-plane slickensides indicates a ductile behaviour in compactional settings (Figs. 12 and 13), and therefore the micro-planes are hydroplastic.

6.1.2. Brittle–ductile transition

Fabric characteristics of Boom Clay indicate that the three types of fractures (micro-planes, meso-planes and joint-related fractures) can be related to compacted ductile shear bands and brittle, dilatant fractures, respectively. Both ductile and brittle failure modes occur very close to each other on different scales ranging from hand sample to microscopic scale. Whether dilatancy or compaction will occur depends on the orientation of the individual fracture strands relative to the stress system, on their position (dilatancy at high strain and ductility in the fracture-tips and at low strain) and on the stress state (see Section 6.4). The transition between ductile and brittle failure is gradual, as we can deduce from the microfabric of some of the joint-wall sections. Sometimes, sub-vertical joints (considered to be 'mode-I' fractures) actually contain a shear component (reorientation of clay particles and formation of secondary shear planes; Fig. 11). These joints are therefore better described as hybrid-type (mixed mode) fractures that form at effectively tensile normal stress levels with differential stress values between 4 and 8 times the tensile strength

Table 4
Brittle versus hydroplastic behaviour

	Brittle behaviour	Hydroplastic behaviour
Mean fault plane	Planar	Often distorted, dislocated
Coating	Polished planes, white patches	Same as country rock
Striae	Well marked and straight	Poorly marked, conical arrays of striae
Secondary structures (shear sense indicators)	Riedel shears dive in the main plane. Grooves of smeared grains. Whitening of striae due to crush of quartz-grains	Riedel shears form step structures. Grooves of smeared grains. More plastic Riedels. Bumpy surfaces
Micro shear-zones	Very thin, micro-breccia	Wider, with grain-size reduction and isolated quartz-grains
Micro-fractures	Tensional micro-cracks	No micro-cracks

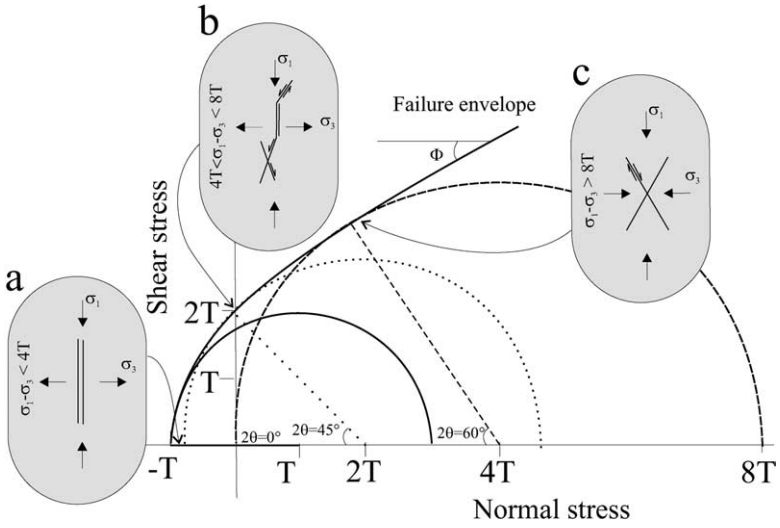

Fig. 15. Mohr-space and schematic real-space representation of: (a) tensile failure; (b) hybrid (mixed mode) failure; and (c) shear failure. T: tensile strength, σ_1: maximum principal compressive stress, σ_3: minimum principal compressive stress, ϕ: angle of internal friction, θ: angle between failure plane and σ_1. After Hancock (1985).

(Fig. 15). Similar secondary structures and combined ductile–brittle failure has been observed on several other samples. Some joints, however, lack the reorientation of particles close to the joint surface and hence are extension features (Fig. 11b).

6.2. Fracture relations

The NW–SE predominant strike of the micro-planes is very close to the prevailing joint-set strike (130°). The other main joint-set strike (30°) is very close to the extension direction (032°; Table 2) and striae azimuth of the slickensides (Figs. 4, 6, 8 and 10). The orientations of the micro-plane slickensides and of the joints are similar to and fit in the same deformation regime as the meso-planes of the Kruibeke fault zone (Figs. 8 and 10). The close geometrical relations suggest a common origin in terms of driving force and deformation evolution.

The changing dynamic settings related to the different fracture types and the cross-cutting relations between the fracture types contain the clue for understanding their subsequent occurrence during the geological history of the clay at different positions on the stress path. The micro-plane related slickensides have been formed in a more radial–tensile stress regime with nearly equal values for both horizontal stresses (Table 2; Figs. 9 and 10), whereas the meso-plane related faults formed in a stress field that was more anisotropic (σ_2 getting significantly larger than σ_3; Table 2; Fig. 9). This is also reflected by the trend distribution of the micro-plane slickensides, which is much more variable than that of the meso-plane faults. These could grow in a system where they were able to develop a strike parallel to the more distinct SH_{max} (σ_2), at the moment that horizontal stress got more anisotropic. The strong anisotropy in joint trend and prevalence of two, mutually perpendicular joint sets also suggests that their formation occurred in a stress system where horizontal stress was anisotropic and SH_{max} was oriented NW–SE, parallel to both the main joint trend (J_1), meso-plane trend and dominant micro-plane trend.

Vertical mode-I fractures (joints) are often closely related to much less dipping micro-plane shear bands with the same strike. Cross-cutting relations between joint planes and meso-planes at the Kruibeke fault zone indicate that the former cuts the latter, suggesting that jointing postdates faulting (Fig. 7b). However, there were various circumstances wherein the chronology could not be distinguished. There is no clear regularity or progressive transition in the spatial (depth-related or laterally confined) occurrences of the different failure-mode related structures. Most likely, the transition from ductile to brittle is controlled by subtle local stress transitions depending on the structural level.

6.3. Mechanical inferences: the brittle/ductile succession

Ductile deformation of clay-rich sediments has been observed in different geological settings. S–C-foliations have been reported in scaly-clay fabrics in ODP related mudstones (Takizawa and Ogawa, 1999). Ductile Riedel-shear and associated simple shear deformation bands were observed in experimentally deformed clays (Tchalenko, 1968; van den Berg, 1987; Arch et al., 1988). The development of those structures has been attributed to the high water content in a confined (relatively high p') system. In the present study, the ductile shear bands probably are to be related to deeper levels of deformation and to higher confining pressure, whereas the dilatant structures develop at low confining pressure, closer to the surface.

In order to form shear bands, a build-up of differential stress is required, the origin of which can be endogenous

(related to material properties) or exogenous (influenced by regional stress changes), or a combination of both. With increasing differential stress, compressional (shear) normal faulting in a brittle regime would allow the formation of the meso-plane related faults. Ongoing horizontal extension would eventually lead to vertical jointing. However, in the absence of external forces, overconsolidated clay will experience during unloading first a reduction in differential stress followed by a swap in principal compressive stress close to the surface, the horizontal stress getting larger then the vertical (depending on the stiffness of the material; see Maltman, 1994). In the case of the Boom Clay, this horizontal compression would start after uplift and unloading to about 50 m below the surface (Mertens et al., 2003). In order to explain the vertical joints in the Boom Clay, horizontal stress has to be reduced and become tensile in some way. Moreover, this has to occur under moderate differential stress in order to prevent shear failure. In the absence of fluid overpressure and assuming K_0 conditions (no tectonic stress, no overconsolidation), a shrinkage mechanism has been proposed to reduce the horizontal stress (Mertens et al., 2003). However, regional tectonism contributed to a flexure-induced slope-parallel horizontal extension (and sub-vertical compression) component during uplift and tilting of overconsolidated Boom Clay, leading to differential stress development. As uplift continues and differential stress increases, the mud exceeds the critical state line and dilation occurs.

The moderately dipping slickensides (dip between 30 and 60°) have formed earlier in the stress path when the normal effective stress (and the 2θ-angle; Fig. 15) was high. The slickensides directly adjoining sub-vertical joints and hybrid-mode shear fractures (Fig. 11) generally dip steeper than 60°. They were formed at lower effective stress levels, closer to the dilatancy boundary (Fig. 13) and hence developed at smaller 2θ-angles relative to the vertical σ_1-axis (Fig. 15).

Based on the above discussed observations, a hierarchy of fracture development is proposed for Boom Clay during burial to and uplift from its deepest position (Fig. 16).

1. The mud is buried, accompanied by compaction and consolidation, following a K_0 stress path up to the pre-consolidation pressure (p'_c; Fig. 16) at the maximal depth of burial. This is for 150 m burial around p'_c = 1.25 MPa (σ'_1 = 1.5 MPa and K_0 = 0.7; see Table 1 for used parameters).
2. Moderately dipping (20° < dip angle < 50°) ductile shear bands (micro-planes) with random orientation are formed, induced by the weak nature of the argillaceous sediments at very small differential stress levels caused by loading-induced endogenous forces and enhanced by uplift-related extensional tectonism. The shear bands formed at the clay's highest confinement state, just before or close after the onset of uplift of buried Boom Clay, where the estimated cohesion is about 175–200 kPa (Wildenborg and Bogdan, 2000), the differential stress in the absence of tectonic stress would be around 0.50 MPa. This is close to the estimated critical state limit of Boom Clay (Schittekat et al., 1983). A slight increase in differential stress (or decrease in mean effective stress) at a depth of 100–150 m will lead to ductile ('wet-side') failure (Figs. 13 and 16). The range of stress change at which this ductile type of deformation will occur in Boom Clay is about 0.5 MPa of mean effective stress change and up to 0.2 MPa of differential stress change (Fig. 16).
3. Steeper dipping (> 50°) slickensides are formed as uplift continues and tectonic differential stress increases. This causes a strong preferred orientation of the slickensides.
4. Meso-planes start to develop under tectonic differential stress. The faults strike perpendicular to the regional extension direction (Fig. 15c).
5. Mixed-mode hybrid joints (Fig. 15b) form when the horizontal stress becomes tensile. Differential stress is reduced by uplift-related reduction of σ_1 (vertical compression) and confining pressure (Fig. 15a).

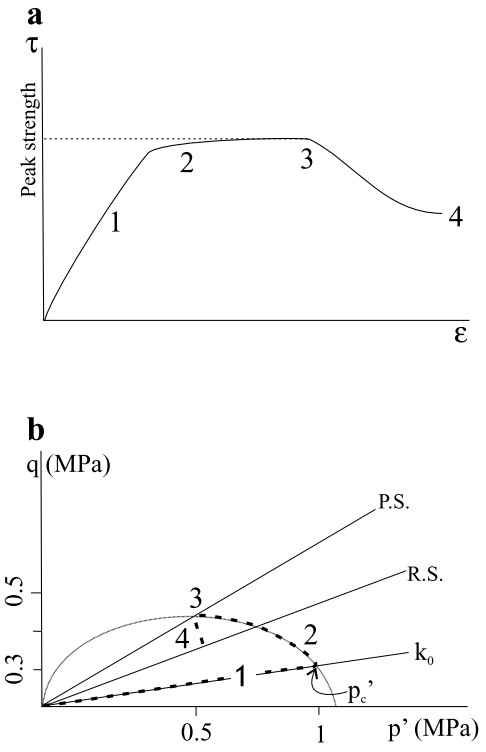

Fig. 16. Model explaining the stress path and related structural evolution of uplifting Boom Clay. (a) Shear stress (τ)–shear strain (ε) diagram illustrating the concept of transitional clay behaviour. 1. Elastic strain path. Deformation by volumetric strain (void ratio reduction). 2. Pre-peak, ductile, 'wet-side' failure. 3. Brittle failure at peak strength. 4. Residual strength. (b) Differential stress (q)–mean effective stress (p') diagram (see Fig. 13 for explanation) illustrating the possible effective stress path followed by the Boom Clay during burial and uplift (dashed line). P.S. = peak strength. R.S. = residual strength, critical state. K_0 = normal consolidation line. p'_c = maximal mean effective pressure. Representative values for Boom Clay are given (after Schittekat et al., 1983 and Table 1).

6. Dilational tensile fractures (J_1 vertical joints) form close to the sediment surface at low confining pressure. Horizontal stresses can locally and temporarily swap and perpendicular joint sets (J_2) develop.

At the onset of uplift, the influence of the far-field stresses is still small and the small differential stress is a result of internal material characteristics of the weak mud. As uplift continues, differential stress gets increasingly more dominated and enhanced by the regional stress. The strength of the rock will also be increased, due to the effect of hardening, embrittlement and overconsolidation (Fig. 17). The initial Mohr-circle is increased up to failure by a decrease in σ_3, caused by the tectonic stress field. Ductile failure can cause the fault rock to harden (by grain compaction and increasing resistance to shear of undulating shear planes) with small loss of cohesion (Fig. 17). In that way, new slip planes develop with increasing differential stress during uplift, rather then reactivation of pre-existing planes (Underhill and Woodcock, 1987). This accounts for the abundance of micro-planes with small offsets.

Lithological controls on fracture partitioning could cause coeval development of faults in mechanically weaker beds (clay) and joints in mechanically stronger (more competent) silt-rich layers (Ferrill and Morris, 2003). In the Boom Clay, the ductile slickensides are more abundant in clay-rich layers than in silt-rich layers, suggesting that differences in competency would influence the failure mode. The relation between jointing and mechanical layering is somewhat different. Most joints transect both clayey and silty layers. They do not seem to be much influenced by strength variations, except for the fracture density, which is higher (smaller spacing) in the clay-rich layers. This supports the idea that the clay-rich layers, more strongly affected by ductile failure, get stiffer than the silt-rich layers after uplift.

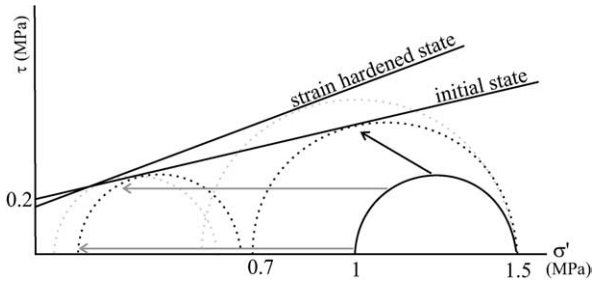

Fig. 17. Mechanism for differential failure in clay. Initial Mohr-circle is displaced to the left by increased pore fluid pressure (grey arrows), or the diameter of the Mohr-circle is increased up to failure by an exogenous tectonic stress or by an endogenous volume reduction (black arrow). Hardened failures envelop after initial failures, causing new, steeper slip-planes to develop. Light-grey, dotted stress circles indicate the additional stress change needed to form new shear planes after hardening. After Underhill and Woodcock (1987) and Goulty (2001).

6.4. Geological inferences

The regional stress and deformation regime during the late Cenozoic in northwestern Europe show a general northwesterly-trending SH_{max} and northeasterly-trending extension direction in a normal faulting regime (Vandycke et al., 1991; Bergerat and Vandycke, 1994; Vandycke, 2002). This regional stress regime can explain why a northeasterly-directed extension direction dominates the deformation of the Boom Clay at all its structural levels. The tectonic extension originates from the uplift of the Ardenne–Rhenish and London–Brabant massifs in the southwest and subsequent flexuring of the southern extremity of the North Sea Basin.

The intraformational nature of the fracturing and the original wide trend-distribution of micro-plane slickensides suggest a combination of endogenous and exogenous stress controlling the observed deformation. The orientation distribution in the micro-plane related slickensides resembles the polygonal fault geometry (Cartwright and Lonergan, 1996; Lonergan et al., 1998; Goulty, 2001). Nevertheless, the variable orientation evolves into a deformational system with consistent horizontal stress axes. The endogenous stress system progressively gets overprinted by a tectonic extension, determining the main orientations of the slickensides and joints.

There is a distinct dominance of south-dipping (Fig. 6, i.e. up-slope regarding the dip of the Boom Clay, Fig. 1) micro-planes in the outcrop area of the Boom Clay. Analogue sandbox models simulated faulting related to gravitational collapse on a tilted slope sequence (Higgs and McClay, 1993). They supported the idea that faults in the Miocene sediments of the North Sea Central Graben result from down-slope gravity sliding and preferentially initiate along up-slope dipping (antithetic) planes. Another example is present in Oligocene deposits in the North Sea, containing intraformational normal faults triggered by down-slope gravity sliding of overpressured mud (Clausen et al., 1999). The development of these faults could well be an analogue to the fractures observed in the Boom Clay.

7. Summary and conclusion

In uncemented argillaceous sediments (mud), a typical brittle–ductile fabric can form during geological evolution. In the present paper, the Boom Clay has been used as an example for assessing fracturing mechanisms in mud. However, elaborating on previous studies on other mud sequences (Bishop et al., 1965; Maltman, 1987; Horseman et al., 1996), similar models can be conceived to understand the relations between slickensides, faults and joints in terms of combined endogenous and exogenous forces. We illustrated that critical state mechanics is a useful tool to explain the successive, but closely related, development of ductile and brittle structures in argillaceous sediments. A

subtle interplay between compaction and consolidation (endogenous forces) on the one hand and uplift and tilt (tectonic forces) on the other hand, triggers the successive development of compacting shear bands, hybrid shear fractures and dilatant fractures, respectively.

In the specific case of the Boom Clay, intraformational fractures result from a combination of consolidation-related volume reduction and the build-up of a specific stress path resulting from burial and subsequent uplift, bringing the sediments close to their critical stress state. The brittle–ductile transitional rheology caused compacting shear bands to develop in close relation to brittle dilatant structures that form along the same stress path at a higher differential stress level. The distinct anisotropy in fracture orientation indicates an influence of the regional tectonic stress field on the stress path governing the deformation of the sediments.

Down-slope gravity sliding, triggered by late Oligocene uplift of the London–Brabant and Ardenne–Rhenish massifs, and associated tilting of the North Sea sediments, caused bedding parallel extension (joints 130°), down-slope (faults strike 130° and dip 45°NE; Figs. 4 and 10) and up-slope dipping shear-planes (slickensides strike 130° and dip 50°SW; Figs. 6 and 10). Mode-I tensile and hybrid mode fractures are constrained to low effective normal stress levels and are not expected to extend deeper than a few decametres. Ductile shear bands are expected to occur over the whole depth range within the Boom Clay formation, which has been in a 'wet-side' deformation state since the onset of uplift (Figs. 13 and 16).

Dilatancy, the process responsible for fracture porosity and permeability increase creating preferential pathways and possible fluid-flow with increase in hydraulic conductivity in an otherwise impermeable mud, is caused by micro-cracking prior to macroscopic failure and by the formation of macroscopic tensional joints. In the case of the Boom Clay, and of many muds with similar moderate subsidence/uplift histories, dilatancy in natural circumstances is restricted to the shallower structural levels of the sediment, whereas the deeper structural levels undergo ductile, compactional deformation.

Acknowledgements

This study was sponsored by ONDRAF/NIRAS (Belgian radioactive waste agency), in collaboration with K.U. Leuven (Belgium), Faculté Polytechnique (Mons, Belgium) and Université de Franche-Comté (Besançon, France). Manuel Sintubin is Research Associate of the Onderzoeksfonds K.U. Leuven (Belgium). Sara Vandycke is Chercheur Qualifié of the F.N.R.S. (Belgium). The manuscript has benefited greatly from the detailed reviews by Janos Urai, Mary Beth Gray and Editor David A. Ferrill.

References

Agar, S.M., Prior, D.J., Behrmann, J.H., 1988. Back-scattered electron imagery of the tectonic fabrics of some fine-grained sediments: implications for fabric nomenclature and deformation processes. Geology 17, 901–904.

Al-Mukhtar, M.A., Belanteur, N., Tessier, D., Vanapalli, S.K., 1996. The fabric of a clay soil under controlled mechanical and hydraulic stress states. Applied Clay Science 11, 99–115.

Al-Shayea, N.A., 2001. The combined effect of clay and moisture content on the behavior of remolded unsaturated soils. Engineering Geology 62, 319–342.

Anderson, E.M., 1951. The Dynamics of Faulting and Dyke Formation with Application to Britain. Oliver & Boyd, Edinburgh.

Angelier, J., 1994. Fault slip analysis and paleostress reconstruction. In: Hancock, P.L. (Ed.), Continental Deformation. Pergamon Press, Bristol, pp. 53–100.

Aplin, A.C., Fleet, A.J., Macquaker, J.H.S., 1999. Muds and mudstones: physical and fluid-flow properties. In: Aplin, A.C., Fleet, A.J., Macquaker, J.H.S. (Eds.), Muds and Mudstones: Physical and Fluid Flow Properties Geological Society Special Publications, 158, pp. 1–8.

Arch, J., Maltman, A.J., 1990. Anisotropic permeability and tortuosity in deformed wet sediments. Journal of Geophysical Research 95, 9035–9045.

Arch, J., Maltman, A.J., Knipe, R.J., 1988. Shear-zone geometries in experimentally deformed clays: the influence of water content, strain rate and primary fabric. Journal of Structural Geology 10, 91–99.

van den Berg, L., 1987. Experimental redeformation of naturally deformed scaly clays. Geologie en Mijnbouw 65, 309–315.

Bergerat, F., Vandycke, S., 1994. Paleostress analysis and geodynamical implications of Cretaceous–Tertiary faulting in Kent and the Boulonnais. Journal of the Geological Society, London 151, 439–448.

Bevan, T.G., Hancock, P.L., 1986. A late Cenozoic regional mesofracture system in southern England and northern France. Journal of the Geological Society, London 143, 355–362.

Bishop, A.W., Webb, D.L., Skinner, A.E., 1965. Triaxial tests of soil at elevated cell pressures. Proceedings of the International Conference on Soil Mechanics, Montreal, 170–174.

Blatt, H., Middleton, G.V., Murray, R.C., 1980. Origin of Sedimentary Rocks. Prentice-Hall, Englewood Cliffs, NJ.

Burland, J.B., Rampello, S., Georgiannou, V.N., Calabresi, G., 1996. A laboratory study of the strength of four stiff clays. Geotechnique 46, 491–514.

Camelbeeck, T., Meghraoui, M., 1996. Large earthquakes in northern Europe more likely than once thought. Eos 77, 405–409.

Camelbeeck, T., Meghraoui, M., 1998. Geological and geophysical evidence for large palaeo-earthquakes with surface faulting in the Roer Graben (northwest Europe). Geophysical Journal International 132, 347–362.

Caputo, R., 1995. Evolution of orthogonal sets of coeval extension joints. Terra Nova 7, 479–490.

Cartwright, J., Lonergan, L., 1996. Volumetric contraction during the compaction of mudrocks: a mechanism for the development of regional-scale polygonal fault systems. Basin Research 8, 183–193.

Clausen, J.A., Gabrielsen, R.H., Reksnes, P.A., Nysaether, E., 1999. Development of intraformational (Oligocene–Miocene) faults in the northern North Sea: influence of remote stresses and doming of Fennoscandia. Journal of Structural Geology 21, 1457–1475.

De Craen, M., Swennen, R., Keppens, E.M., Macauley, C.I., Kiriakoulakis, K., 1999. Bacterially mediated formation of carbonate concretions in the Oligocene Boom Clay of northern Belgium. Journal of Sedimentary Research 69, 1098–1106.

Dehandschutter, B., 2001. Study of the recent structural evolution of continental basins in Altai-Sayan (Central Asia). PhD thesis, Vrije Universiteit Brussel.

Dehandschutter, B., Sintubin, M., Vandenberghe, N., Vandycke, S., Gaviglio, P., Wouters, L., 2002. Fracture analysis in the Boom Clay (URF, Mol, Belgium). Aardkundige Mededelingen 12, 245–248.

Dehandschutter, B., Vandycke, S., Sintubin, M., Vandenberghe, N., Gaviglio, P., Sizun, J.-P., Wouters, L., 2004. Microfabric of fractured Boom Clay at depth: a case study of brittle–ductile transitional clay behaviour. Applied Clay Science 26, 389–401.

Delvaux, D., Moeys, D., Stapel, R., Petit, C., Levi, K., Miroshnichenko, A., Ruzhich, V., San'kov, V., 1997. Paleostress reconstructions and geodynamics of the Baikal region, Central Asia, Part 2: Cenozoic rifting. Tectonophysics 282, 1–38.

Dirkzwager, J.B., van Wees, J.D., Cloetingh, S., Geluk, M.C., Dost, B., Beekman, F., 2000. Geo-mechanical and rheological modelling of upper crustal faults and their near-surface expression in the Netherlands. Global and Planetary Change 27, 67–88.

Dunne, W.M., Hancock, P.L., 1994. Paleostress analysis of small-scale brittle structures. In: Hancock, P.L. (Ed.), Continental Deformation. Pergamon Press, Bristol, pp. 101–118.

EURIDICE News Nr 2., 2003. http://www.euridice.be

Faas, R.W., Crockett, D.S., 1983. Clay fabric development in a deep-sea core. Site 515. Deep Sea Drilling Project Leg 72, Initial Rep. DSDP 72, 519–525.

Ferrill, D.A., Morris, A.P., 2003. Dilational normal faults. Journal of Structural Geology 25, 183–196.

Goulty, N.R., 2001. Mechanics of layer-bound polygonal faulting in fine-grained sediments. Journal of the Geological Society, London 159, 239–246.

Gray, M.B., Nickelsen, R.P., 1989. Pedogenic slickensides, indicators of strain and deformation processes in redbed sequences of the Appalachian foreland. Geology 17, 72–75.

Guiraud, M., Séguret, M., 1987. Soft-sediment microfaulting related to compaction within the fluvio-deltaic infill of the Soria strike-slip basin (northern Spain). In: Jones, M.E., Preston, R.M.F. (Eds.), Deformation of Sediments and Sedimentary Rocks Geological Society Special Publications 29, London, pp. 123–136.

Hancock, P.L., 1985. Brittle microtectonics: principles and practice. Journal of Structural Geology 7, 437–457.

Hancock, P.L., AL-Kadhi, A., Barka, A.A., Bevan, T.G., 1987. Aspects of analysing brittle structures. Ann. Tectonicae 1, 5–19.

Henriet, J.P., De Batist, M., Verschuren, M., 1991. Early fracturing of Palaeogene clays, southernmost North Sea: relevance to mechanisms of primary hydrocarbon migration. In: Spencer, A.M. (Ed.), Generation, Accumulation, and Production of Europe's Hydrocarbons. Oxford University Press, Oxford, pp. 217–227.

Higgs, W.G., McClay, K.R., 1993. Analogue sandbox modelling of Miocene extensional faulting in the outer Moray Firth. In: Williams, G.D., Dobb, A. (Eds.), Tectonics and Seismic Sequence Stratigraphy Geological Society Special Publications 71, London, pp. 141–162.

Hoeppener, R., 1955. Tektonik im Schiefergebirge. Geologische Rundschau 44, 26–58.

Horseman, S.T., Winter, M.G., Entwistle, D.C., 1987. Geotechnical characterization of Boom Clay in relation to the disposal of radioactive waste. EUR 10987, Commission of the European Communities 1987.

Horseman, S.T., McCann, D.M., McEwan, T.J., Brightman, M.A., 1996. Determination of the geotechnical properties of mudrock from geophysical logging of the Harwell boreholes. FLPU 84-14. British Geological Survey. Fluid Processes Research Group.

Ingram, G.M., Urai, J.L., 1999. Top-seal leakage trough faults and fractures: the role of mudrock properties. In: Aplin, A.C., Fleet, A.J., Macquaker, J.H.S. (Eds.), Muds and Mudstones: Physical and Fluid Flow Properties Geological Society Special Publications 158, London, pp. 125–135.

Jones, M.E., Addis, M.A., 1985. On the changes in porosity and volume during a burial of argillaceous sediments. Marine and Petroleum Geology 2, 247–252.

Jones, M.E., Addis, M.A., 1986. The application of stress path and critical state analysis to sediment deformation. Journal of Structural Geology 8, 575–580.

Labiouse, V., Bernier, F., 1997. Hydro-mechanical disturbances around excavations. In: Feasibility and Acceptability of Nuclear Waste Disposal in the Boom Clay Formation. SCK-CEN Report, pp. 15–34.

Laenen, B., 1999. The geochemical signature of relative sea-level cycles recognised in the Boom Clay. Aardkundige Mededelingen 9, 61–82.

Letsch, W.J., Sissingh, W., 1983. Savian erosion. Geologie en Mijnbouw 62, 305–318.

Lockner, D.A., Byerlee, J.D., Kuksenko, V., 1992. Observations of quasistatic fault growth from acoustic emissions. In: Evans, B., Wong, T.-F. (Eds.), Fault Mechanics and Transport Properties of Rocks. Academic Press, San Diego, pp. 1–31.

Lonergan, L., Cartwright, J., Jolly, R., 1998. The geometry of polygonal fault systems in Tertiary mudrocks of the North Sea. Journal of Structural Geology 20, 529–548.

Maltman, A.J., 1984. On the term soft-sediment deformation. Journal of Structural Geology 6, 589–592.

Maltman, A.J., 1987. Microstructures in deformed sediments, Denbigh Moors, North Wales. Geological Journal 22, 87–94.

Maltman, A.J., 1994. The Geological Deformation of Sediments. Chapman & Hall, London.

Mandl, G., 1999. Faulting in Brittle Rocks. Springer, Berlin.

Means, W.D., 1987. A newly recognised type of slickenside striation. Journal of Structural Geology 9 (5/6), 585–590.

Meghraoui, M., Camelbeeck, T., Vanneste, K., Brondeel, M., Jongmans, D., 2000. Active faulting and paleoseismology along the Bree fault, lower Rhine graben, Belgium. Journal of Geophysical Research 105, 13809–13841.

Menéndez, B., Zhu, W., Wong, T.-F., 1996. Micromechanics of brittle faulting and cataclastic flow in Berea sandstone. Journal of Structural Geology 18, 1–16.

Mertens, J., Vandenberghe, N., Wouters, L., Sintubin, M., 2003. The origin and development of joints in the Boom Clay Formation (Rupelian) in Belgium. In: Van Rensbergen, P., Hillis, R.R., Maltman, A.J., Morley, C.K. (Eds.), Subsurface Sediment Mobilization Geological Society Special Publications 217, London, pp. 311–323.

Mertens, J., Bastiaens, W., Dehandschutter, B., 2004. Characterisation of induced discontinuities in the Boom Clay around the underground excavations (URF, Mol, Belgium). Applied Clay Science 26, 413–428.

Michon, L., Van Balen, R.T., Merle, O., Pagnier, H., 2003. The Cenozoic evolution of the Roer Valley Rift System integrated at a European scale. Tectonophysics 367, 101–126.

Morgenstern, N.R., Tchalenko, J.S., 1967. Microscopic studies of Kaolin subjected to direct shear. Geotechnique 17, 309–328.

Müller, B., Zoback, M.L., Fuchs, K., Mastin, L., Gregersen, S., Pavoni, N., Stephansson, O., Ljunggren, C., 1992. Regional patterns of tectonic stress in Europe. Journal of Geophysical Research 97 (B8), 11783–11803.

Ngwenya, B.T., Elphick, S.C., Main, I.G., Shimmield, G.B., 2000. Experimantal constraints on the diagenetic self-sealing capacity of faults in high porosity rocks. Earth and Planetary Science Letters 183, 187–199.

ONDRAF/NIRAS, 2001. Safety Assessment and Interim Report No. 2. Brussels, NIROND 2001-06 E.

Paulissen, E., 1997. Quaternary morphotectonics in the Belgian part of the Roer Graben. Aardkundige Mededelingen 8, 131–134.

Petit, J.P., Laville, E., 1987. Morphology and microstructures of hydroplastic slickensides in sandstone. In: Jones, M.E., Preston, R.M.F. (Eds.), Deformation of Sediments and Sedimentary Rocks Geological Society Special Publications 29, London, pp. 107–121.

Petley, D.N., 1999. Failure envelope of mudrocks at high confining pressures. In: Aplin, A.C., Fleet, A.J., Macquaker, J.H.S. (Eds.), Muds and Mudstones: Physical and Fluid Flow Properties Geological Society Special Publications 158, London, pp. 61–71.

Pouya, A., Djéran-Maigre, I., Lamoureux-Var, V., Grunberger, D., 1998. Mechanical behaviour of fine grained sediments: experimental compaction and three-dimensional constitutive model. Marine and Petroleum Geology 15, 129–143.

Rogers, S.F., 2003. Critical stress-related permeability in fractured rocks. In: Ameen, M. (Ed.), Fracture and In-Situ Stress Characterisation of Hydrocarbon Reservoirs Geological Society Special Publications 209, London, pp. 7–16.

Romero, E., Gens, A., Lloret, A., 1999. Water permeability, water retention and microstructure of unsaturated compacted Boom clay. Engineering Geology 54, 117–127.

Rutter, E.H., 1986. On the nomenclature of mode of failure transition in rocks. Tectonophysics 122, 381–387.

Rutter, E.H., Hadizadeh, J., 1991. On the influence of porosity on the low-temperature brittle–ductile transition in siliciclastic rocks. Journal of Structural Geology 13, 609–614.

Schittekat, J., Henriet, J.P., Vandenberghe, N., 1983. Geology and geotechnique of the Scheldt Surge Barrier. Characteristics of an overconsolidated clay. 8th International Harbour Congress 2, 121–135.

Sibson, R.H., 1981. Controls on low-stress hydro-fracture dilatancy in thrust, wrench and normal fault terrains. Nature 289, 665–667.

Sibson, R.H., 2000. Fluid involvement in normal faulting. Journal of Geodynamics 29, 469–499.

Sintubin, M., Sels, O., Buffel, P., 2002. Late Tertiary fault activity in the southwestern boundary fault system of the Roer Valley Graben: evidences from the Bree area (NE Belgium). Geologie en Mijnbouw 80, 69–78.

Skempton, A.W., 1964. Long-term stability of clay slopes. Geotechnique 14, 77–114.

Takizawa, S., Ogawa, Y., 1999. Dilatant clayey microstructure in the Barbados décollement zone. Journal of Structural Geology 21, 117–122.

Tchalenko, J.S., 1968. The evolution of kink-bands and the development of compression textures in sheared clays. Tectonophysics 6, 159–174.

Underhill, J.R., Woodcock, N.H., 1987. Faulting mechanisms in high-porosity sandstones; New Red Sandstone, Arran, Scotland. In: Jones, M.E., Preston, R.M.F. (Eds.), Deformation of Sediments and Sedimentary Rocks Geological Society Special Publications 29, London, pp. 91–105.

Van Echelpoel, E., Weedon, G.P., 1990. Milankovich cyclicity and the Boom Clay Formation: an Oligocene siliciclastic shelf sequence in Belgium. Geological Magazine 127, 599–604.

Vandenberghe, N., 1978. Sedimentology of the Boom Clay (Rupelian) in Belgium: Brussel Verhandeling Koninklijke Academie voor Wetenschappen, 147, Verhandelingen Koninklijke Academie voor Wetenschappen, Letteren en Schone Kunsten van België, Klasse der Wetenschappen, Brussel 1978.

Vandenberghe, N., Laenen, B., Van Echelpoel, E., Lagrou, D., 1997. Cyclostratigraphy and climatic eustasy. Example of the Rupelian stratotype. Comptes Rendus de L'Académie des Sciences—Earth and Planetary Science 325, 305–315.

Vandenberghe, N., Laga, P., Steurbaut, E., Hardenbol, J., Vail, P., 1998. Tertiary sequence stratigraphy at the southern border of the North Sea Basin in Belgium. In: de Graciansky, P.C., Hardenbol, J., Jacquin, Th., Vail, P.R. (Eds.), Mesozoic and Cenozoic Sequence Stratigraphy of European Basins SEMP Special Publication No. 60, pp. 119–154.

Vandycke, S., 2002. Paleostress records in Cretaceous formations in NW Europe: extensional and strike-slip events in relationships with Cretaceous–Tertiary inversion tectonics. Tectonophysics 357, 119–136.

Vandycke, S., Bergerat, F., Dupuis, Ch., 1991. Meso-Cenozoic faulting and inferred palaeostresses in the Mons Basin, Belgium. Tectonophysics 192, 261–271.

Wildenborg, T., Bogdan, O., 2000. Transport of radionuclides through a clay barrier. TNO-NITG Information, December 2000, pp.8–12.

Wong, T.F., David, C., Zhu, W., 1997. The transition from brittle faulting to cataclastic flow in porous sandstones; mechanical deformation. Journal of Geophysical Research (B) 102, 3009–3025.

Wood, D.M., 1990. Soil Behaviour and Critical State Soil Mechanics. Cambridge University Press, Cambridge, UK.